Methamphetamine withdrawal induces activation of CRF neurons in the brain stress system in parallel with an increased activity of cardiac sympathetic pathways

Juan Antonio García-Carmona[1,2*] juanantonio.garcia8@um.es,
Polymnia Georgiou[3,4],
Panos Zanos[3,4],
Alexis Bailey[3,5],
Maria Luisa Laorden[1]

[1]Department of Pharmacology, Faculty of Medicine
University of Murcia
Murcia, Spain

[2]Unit of Acute Psychiatry
Reina Sofía University Hospital
Av Intendente Jorge Palacios 1, 30003 Murcia, Spain

[3]Department of Biochemistry, Faculty of Health and Medical Sciences
University of Surrey
Guildford, UK

[4]Department of Psychiatry
University of Maryland School of Medicine
Baltimore, MD 21209, USA

[5]Institute of Medical and Biomedical Education
St. George's University of London
London SW17 0R, UK

Abstract

Methamphetamine (METH) addiction is a major public health problem in some countries. There is evidence to suggest that METH use is associated with increased risk of developing cardiovascular problems. Here, we investigated the effects of chronic METH administration and withdrawal on the activation of the brain stress system and cardiac sympathetic pathways. Mice were treated with METH (2 mg/kg, i.p.) for

10 days and left to spontaneous withdraw for 7 days. The number of corticotrophin-releasing factor (CRF), c-Fos, and CRF/c-Fos neurons was measured by immunohistochemistry in the paraventricular nucleus of the hypothalamus (PVN) and the oval region of the bed nucleus of stria terminalis (ovBNST), two regions associated with cardiac sympathetic control. In parallel, levels of catechol-*o*-methyl-transferase (COMT), tyrosine hydroxylase (TH), and heat shock protein 27 (Hsp27) were measured in the heart. In the brain, chronic-METH treatment enhanced the number of c-Fos neurons and the CRF neurons with c-Fos signal (CRF^{+}/$c\text{-}Fos^{+}$) in PVN and ovBNST. METH withdrawal increased the number of CRF^{+} neurons. In the heart, METH administration induced an increase in soluble (S)-COMT and membrane-bound (MB)-COMT without changes in phospho (p)-TH, Hsp27, or pHsp27. Similarly, METH withdrawal increased the expression of S- and MB-COMT. In contrast to chronic treatment, METH withdrawal enhanced levels of (p)TH and (p)Hsp27 in the heart. Overall, our results demonstrate that chronic METH administration and withdrawal activate the brain CRF systems associated with the heart sympathetic control and point towards a METH withdrawal induced activation of sympathetic pathways in the heart. Our findings provide further insight in the mechanism underlining the cardiovascular risk associated with METH use and proposes targets for its treatment.

Juan Antonio García-Carmona and Polymnia Georgiou contributed equally to this work

Keywords

Methamphetamine
Addiction
Withdrawal
CRF
COMT
Hsp27
Heart

Introduction

Methamphetamine (METH), or methylamphetamine, the N-methylated analogue of the psychostimulant amphetamine is widely abused in certain countries (Panenka et al. 2013). METH use is extensive because of its relatively easy clandestine manufacture and low street cost and the health consequences of METH addiction are devastating (Gonzales et al. 2010; for review, see Wada 2011). Nonetheless, currently, there is no available pharmacotherapy for METH addiction (Ciccarone 2011).

Acutely, METH induces euphoric effects via the stimulation of dopamine, noradrenaline, and 5-hydroxytryptamine release in neurons of the brain through amine redistribution from synaptic vesicles to the cytoplasm and by reversing the action of monoamine transporters (Krasnova and Cadet 2009; Sulzer et al. 2005). Chronic use of METH leads to neurotoxic effects, e.g., degeneration of striatal dopaminergic neurons (Wagner et al. 1980), the formation of reactive oxygen species (Cubells et al. 1994; LaVoie and Hastings 1999; O'Dell et al. 1991; Yamamoto and Zhu 1998), and/or glutamate excitotoxicity as a consequence of METH-induced glutamate release in the striatum (Abekawa et al. 1994; Nash and Yamamoto 1992; Stephans and Yamamoto 1994). In addition to the neurotoxic effects of METH, its use also causes adverse and potentially fatal effects on the cardiovascular system (for review, see Kaye et al. 2007). Specifically, chronic METH exposure is linked to a wide variety of cardiovascular disorders associated with impaired heart rate and vagal abnormalities, including tachycardia, hypertension, cardiomyopathy, coronary artery disease, prolonged QTc interval, and myocardial infarction (Ito et al. 2009; Henry et al. 2012).

Similar to stress, METH withdrawal leads to the activation of the catecholaminergic system resulting in enhanced circulating catecholamine levels, which were shown to induce microfocal fibrosis damage of the heart (Kasch 1987). Noradrenergic neurons projecting from the brainstem are directly responsible for the sympathetic activation of the nervous system, including cardiovascular regulation through spinal cord innervations (Sawchenko and Swanson 1982). Neuronal firing rate in the brainstem is mediated by the activation of corticotrophin-releasing factor (CRF) fibers that project from the paraventricular nucleus of the hypothalamus (PVN) and the oval region of the bed nucleus of the stria terminalis (ovBNST) to the noradrenergic neurons located in the solitary tract and ventrolateral medulla (Stamatakis et al. 2014), thus implicating a key role for CRF in sympathetic cardiovascular regulation. In addition, the PVN and the ovBNST receive afferent projections from several limbic structures that are implicated in behavioral/stress-related responses, as well as cardiovascular control, such as the medial amygdala, the prefrontal cortex, and the lateral septum (Risold and Swanson 1997; Ongur et al. 1998, Daniel and Rainnie 2016).

The role of CRF in several brain regions including the amygdala, hypothalamus, septum, and BNST in drug addiction and stress regulation, as well as their interaction, has been well documented (Koob 2010). Nonetheless, the specific regulation of CRF in METH-induced cardiac alterations remains undetermined. Thus, given the severe

Deleted: ;

Deleted: '

Deleted: or/

Deleted:

cardiovascular complications associated with chronic METH use, the investigation of the neuropathophysiology underlining the cardiovascular consequences of chronic METH use is warranted to shed light in the mechanism linking the CRF stress systems in brain regions associated with cardiovascular sympathetic control such as the PVN and the ovBNST with heart complications.

Therefore, in the present study, we have evaluated the effects of chronic METH-treatment and spontaneous withdrawal in the CRF stress system in the PVN and the ovBNST in brain. We firstly measured the number of neurons expressing CRF and/or c-Fos in both brain areas following chronic METH administration and withdrawal. In addition, we assessed biochemical markers of sympathetic activation including soluble (S) and membrane-bound (MB)-catechol-*o*-methyl transferase (COMT), enzyme involved in the degradation of catecholamine, and tyrosine hydroxylase (TH) phosphorylated at Ser40 (THpSer40), the limiting enzyme in catecholamine synthesis, in the left ventricle of the heart. Moreover, levels of the heat shock protein (Hsp27) and the phosphorylated protein at serine 82 (pHSP27), which protect cells under stress conditions, were measured in the left ventricle. The left ventricle was selected as it receives sympathetic innervations from brainstem regions innervated by CRF neurons localized in PVN and ovBNST.

Materials and methods

Animals

Male C57BL/6J mice (7 weeks old, 20–25 g, Charles River Laboratories, Kingston, UK) were housed in groups of three to four animals per box in a temperature-controlled environment with a 12-h light/dark cycle (lights on 06:00 a.m.). Food and water were available ad libitum. Mice were left to acclimatize in their new environment for 7 days prior to the experimental start and were handled daily by the experimenter. All experimental procedures were conducted in accordance with the UK Animal Scientific Procedures Act (1986).

Drugs and chemicals

Methamphetamine was obtained from Sigma-Aldrich (Poole, UK); sodium dodecyl sulfate, polyacrylamide gel, and PVDF membranes were obtained from Bio-Rad Laboratory (Teknovas, Bilbao, Spain); and goat serum and nickel sulfate were from Sigma Aldrich (St. Louis, MO).

Deleted: *0*

Deleted:

Deleted: M

Deleted: -

Deleted: -

Deleted: ,

Deleted: 3–4

Deleted: hou

Deleted: :

Deleted: -

Deleted: seve

Deleted: .

Deleted: .

Deleted: C

Deleted: dod

Deleted: (

Deleted: ,

Chronic steady-dose methamphetamine administration paradigm

Mice were randomly divided into four groups: saline-, METH-treated, saline-withdrawn, and METH-withdrawn animals. Chronic METH-treated animals were injected i.p. for 10 days with METH (2 mg/kg) (Sigma-Aldrich, Poole, UK), once per day (at 09:00 a.m.), in accordance with Georgiou et al. (2016). The chronic saline-treated group was administered saline (10 ml/kg, i.p.) for 10 days, once per day (at 09:00 a.m.). Saline- and METH-withdrawn animals were treated with the same administration paradigm and left to spontaneously withdrawal for 7 days in their home cages without any injections. Body weights of the animals were measured daily prior to drug treatment and during the withdrawal period at the same time of day. Mice were euthanized by a brief (30 s) exposure to CO_2 1 h post-final injection for the chronic METH/saline administration groups or 7 days post-final injection for the withdrawal groups. The brains and hearts were rapidly removed, fresh-frozen, and immediately stored at − 80 °C until use for Western blot analysis, and immunohistochemistry quantification.

Hematoxylin and eosin staining for heart tissue sections

To assess cardiac histology, the hematoxylin and eosin staining of heart tissue sections was used. Hearts were fixed in 10% neutral buffered formalin, dehydrated, and embedded in paraffin wax. Hearts were sectioned (5 µm thick) using a microtome (Reichert Jung 2040 Autocut) and stained with hematoxylin (Sigma Aldrich, Poole, UK) and eosin (VWR International Ltd., Poole, UK). Sections were examined for morphological changes such as hypertrophy, edema, and inflammatory cell infiltrate, and images were obtained by a light microscope. Analysis was performed by an experimenter blind to the treatment groups.

Western blot analysis

Western blot analysis was performed for THpSer40, COMT, total Hsp27, and Hsp27 phosphorylated at Ser82. Left ventricles of the hearts were dissected and were homogenized for 30 s using a homogenization buffer [phosphate-buffered saline, 2%

Deleted: ;
Deleted:
Deleted:
Deleted: AM
Deleted:
Deleted:
Deleted:
Deleted: 00A
Deleted:
Deleted: -
Deleted: sec
Deleted:
Deleted: -
Deleted: B
Deleted: Hae
Deleted: E
Deleted: haer
Deleted: tick
Deleted: haer
Deleted: o
Deleted: B
Deleted:
Deleted: sec
Deleted:

sodium dodecylsulfate (SDS), protease inhibitors (Roche, Germany), and phosphatase inhibitors (Calbiochem, Germany)]. Then, the samples were centrifuged at 10,000×*g* for 10 min at 4 °C. Total protein concentrations were determined spectrophotometrically using the bicinchoninic acid method (Wiechelman et al. 1988). The optimum amount of protein to be loaded was determined in preliminary experiments by loading gels with increasing protein contents (25 to 100 mg) from samples of each experimental group. Equal amounts of protein (50 mg/lane) from each sample were loaded on a 10% SDS polyacrylamide gel (SDS-PAGE), electrophoresed, and transferred onto a polyvinylidenedifluoride (PVDF) membrane using a Mini Trans-Blot Electrophoresis Transfer Cell (Bio-Rad Lab., CA, USA). Non-specific binding of the antibodies was blocked by incubating the membranes in 1% bovine serum albumin (BSA) in Tris buffer saline Tween (TBST, 10 mM Tris–HCl, pH 7.6, 150 mM NaCl, 0.05% Tween 20). The blots were incubated overnight at 4 °C, with the following primary antibodies: polyclonal anti-TH phospho-Ser40 (1:500 dilution; AB5935, Millipore, USA), monoclonal anti-COMT (1:5000 dilution AB5873, Chemicon International, Temecula, MA, USA), polyclonal anti-total Hsp27 (1:500 dilution; sc-1048, Santa Cruz Biotechnology, Santa Cruz, CA, USA), and polyclonal anti-phospho-Ser^{82} Hsp27 (1:500 dilution; ab39399, Abcam Ltd., Cambridge, UK) in TBST with BSA. After three 10-min washings with TBST, the membranes were incubated with the corresponding peroxidase-labeled secondary antibodies for 1 h, at room temperature (anti-goat sc-2350 for total Hsp27; anti-rabbit sc-2004 for Hsp27 phosphorylated at Ser 82 and TH phospho-Ser40; anti-mouse sc-2005 for COMT, Santa Cruz) at 1:5000 dilutions (Santa Cruz, USA). After washing with TBST, immunoreactivity was detected with an enhanced chemiluminescent Western blot detection system (ECL Plus, GE Healthcare, UK) and visualized by a Typhoon 9410 Variable Mode Imager (GE Healthcare). We used anti-total TH (1:1000 dilution; 62 kDa, AB152, Millipore, USA) and β-actin (1:1000 dilution, 45 kDa, Cell Signaling Technology, Inc., Beverly, MA, USA) as our loading control for all experiments and to obtain the ratios. Before re-probing, blots were stripped by incubation with stripping buffer (glycine 25 mM and SDS 1%, pH 2), for 1 h at 37 °C. Blots were subsequently reblocked and probed with total TH or B-actin overnight at room temperature. The ratio of Hsp27 (27 kDa)/B-actin, Hsp27 phosho-Ser82 (27 kDa)/B-actin, TH phospho-Ser40 (60 kDa)/total TH, S-COMT (25 kDa)/B-actin, and MB-COMT (30 kDa)/B-actin were plotted and analyzed by densitometry (AlphaImager, Nucliber, Madrid, Spain). Experimental and control samples were

Deleted: *x*
Deleted:
Deleted: o
Deleted:
Deleted:
Deleted: Cali
Deleted: tris
Deleted: twe
Deleted: :
Deleted:
Deleted: -
Deleted:
Deleted:
Deleted: Biot
Deleted:
Deleted:
Deleted: r
Deleted: w
Deleted: v
Deleted: m
Deleted:
Deleted:
Deleted:
Deleted:
Deleted:
Deleted:
Deleted:
Deleted:
Deleted:
Deleted:

included in the same blots, and relative variations between bands were calculated in the same image.

Double-labeling immunohistochemistry of c-Fos- and CRF-positive neurons in the PVN and ovBNST

Frozen brains were sectioned (20 µm thick; 300 µm apart) using a cryostat (Zeiss Microm 505E, Hertfordshire, UK) as previously described (Georgiou et al. 2015). For c-Fos/CRF double-label immunohistochemistry, PVN and ovBNST tissue sections from each mouse in each treatment group were processed as previously described (Garcia-Carmona et al. 2013). Briefly, sections were incubated in primary rabbit anti-(c-Fos) (1:10,000 dilution; non-cross-reactive with Fos-B, Fra-1 or Fra-2; sc-52; Santa Cruz) and rabbit anti-CRF (1:500 dilution, a gift from Wylie Vale, The Salk Institute, USA) overnight at room temperature. After the primary anti-body incubation period, sections were incubated with the secondary anti-rabbit IgG (diluted 1:1000; Vector Laboratories). Antigens were visualized by a conventional avidin–biotin–immunoperoxidase protocol using reagents from the Vectastain ABC Elite Kit (Vector Laboratories, Burlingame, CA) and 3,3′-diaminobenzidine (DAB) (Sigma Chemical, Madrid, Spain) as chromogen. c-Fos was visualized by using a mixture of $NiSO_4 \cdot 6H_2O$ (33.2 mg/ml), DAB (0.033%), and 0,014% H_2O_2 in 0,175 M sodium acetate solution (pH 7.5). The CRF–antibody–peroxidase complex was stained on 0.033% DAB and $0.014H_20_2$ in 0.05 M Tris–HCl buffer. Tissue sections were transferred into Milli-Q water (Millipore) to stop the color reaction. Sections were dehydrated through graded alcohols cleared in xylene and cover slipped with DPX.

Co-localization of c-Fos immunoreactivity with CRF-positive neurons

Images of brain sections were captured using a video camera (DFC 290; Leica, Madrid, pain) on a light microscope (DM4000B; Leica) at × 20 and × 40 magnifications. The number of c-Fos and CRF immunoreactive neurons was counted by an observer blind to the treatment groups, using a computer-assisted image analysis system (QWIN; Leica) with an identical rectangular frame. Eight to ten sections from each mouse were counted bilaterally at distinct rostro-caudal levels of PVN or ovBNST obtaining an average. c-

Deleted: labe
Deleted:
Deleted:
Deleted:
Deleted:
Deleted: .
Deleted: .
Deleted:
Deleted: ,
Deleted:
Deleted:
Deleted: -
Deleted: -
Deleted:
Deleted: -
Deleted: Cor
Deleted:

Fos-positive expression was identified as cells with dark blue deposits in the nucleus. CRF positive staining was shown as a brown cytoplasmic deposit. Double-labeled CRF/c-Fos neurons were counted in PVN and ovBNST. The CRF-positive cells without a visible nucleus (c-Fos-negative CRF cells) were also included in the analysis. A square field (129 µm) was superimposed on captured image for using as reference area.

Statistical analysis

All the statistical analyses were performed using GraphPad Prism 6.0, and the results are expressed as the mean ± S.E.M. Data from all experiments were analyzed by two-way ANOVA with treatment (saline, methamphetamine) and phase (chronic/withdrawal) as independent variables. ANOVAs were followed by Holm–Sidak *post-hoc* test when significance was reached. Body weight changes were analyzed with repeated measures two-way ANOVA with factors "body weight" and "time (repeated factor)." Significance was set at $p < 0.05$.

Results

Effects of chronic methamphetamine and/or withdrawal on histopathological measures

Histopathological examination of the heart revealed no morphological changes on the heart wall such as hypertrophy, which was calculated by the ratio of heart weight/body weight, edema, and inflammatory cell infiltrate following chronic METH administration and withdrawal (Fig. 1a–d).

Effects of chronic methamphetamine and/or withdrawal on body and heart weights

Body weight of the animals was measured during the chronic METH administration and withdrawal. Two-way repeated measures ANOVA revealed no significant METH-induced alterations on body weights during the chronic administration paradigm, as well as following withdrawal (treatment $F_{[1,22]} = 0.2501$, $p > 0.05$; Fig. 1e). Heart weights were measured following euthanasia, and the relative heart weight was calculated as the ratio of heart/terminal body weight for each animal. Two-way ANOVA revealed no

significant differences between groups on the relative heart weights (phase $F_{[1,23]} = 0.0399$, $p > 0.05$; treatment $F_{[1,23]} = 0.907$, $p > 0.05$; Fig. 1f).

Number of c-Fos-/CRF-positive neurons following chronic methamphetamine and withdrawal in the PVN and ovBNST

Changes in the number of c-Fos$^+$/CRF$^+$ neurons in the PVN (Fig. 2) and ovBNST (Fig. 3) were assessed using immunohistochemistry. Two-way ANOVA on the number a CRF$^+$ neurons in the PVN revealed a significant effect of "treatment" ($F_{[1,20]} = 40.26$, $p < 0.001$), "withdrawal" ($F_{[1,20]} = 12.00$, $p < 0.01$), and "interaction" ($F_{[1,20]} = 7.79$, $p < 0.05$). Holm–Sidak *post-hoc* test showed that METH withdrawal increases the number of CRF$^+$ neurons compared to saline withdrawal ($p < 0.001$) and chronic METH administration ($p < 0.01$) (Fig. 2e). Two-way ANOVA on the c-Fos$^+$ neurons in the PVN revealed a main effect of METH treatment ($F_{[1,20]} = 19.93$, $p < 0.01$) and withdrawal ($F_{[1,20]} = 5.11$, $p < 0.05$). *Post-hoc* test showed an increased ($p < 0.01$) number of c-Fos$^+$ neurons after chronic METH treatment versus saline treatment and spontaneous METH withdrawal (Fig. 2f). Two-way ANOVA on the number of c-Fos$^+$/CRF$^+$ neurons revealed a main effect of METH treatment ($F_{[1,20]} = 24.82$, $p < 0.001$) and withdrawal ($F_{[1,20]} = 9{,}26$, $p < 0.01$). *Post-hoc* test revealed that METH treatment and withdrawal enhanced ($p < 0.001$) the number of CRF$^+$/c-Fos$^+$ neurons. The increase in the number of CRF$^+$/c-Fos$^+$ neurons was higher ($p < 0.001$) after spontaneous withdrawal versus METH treatment (Fig. 2g).

In the ovBNST (Fig. 3), two-way ANOVA on the number a CRF$^+$ neurons revealed a significant effect of treatment ($F_{[1,20]} = 15.24$, $p < 0.001$), withdrawal ($F_{[1,20]} = 14.13$, $p < 0.01$), and interaction ($F_{[1,20]} = 10.43$, $p < 0.01$). Holm–Sidak *post-hoc* test showed that METH withdrawal increases the number of CRF$^+$ neurons compared to saline withdrawal ($p < 0.001$) and chronic METH administration ($p < 0.001$) (Fig. 3e). Two-way ANOVA on the number a c-Fos$^+$ (Fig. 3f) revealed a main effect of treatment ($F_{[1,20]} = 5.90$, $p < 0.05$), withdrawal ($F_{[1,20]} = 12.99$, $p < 0.01$), and interaction ($F_{[1,20]} = 7.59$, $p < 0.05$). *Post-hoc* test indicates a significant ($p < 0.01$) increase of c-Fos$^+$ neurons in the chronic METH group versus saline treatment and spontaneous METH withdrawal (Fig. 3f). Two-way ANOVA on the number a c-Fos$^+$/CRF$^+$ revealed a main effect of treatment ($F_{[1,20]} = 24.82$, $p < 0.0001$) and withdrawal ($F_{[1,20]} = 9.25$, $p < 0.01$). *Post-hoc* test revealed that METH treatment and withdrawal enhanced

Deleted: P…
Deleted: T
Deleted: ure
Deleted: F
Deleted:
Deleted: ure
Deleted:
Deleted: ure
Deleted:
Deleted: '…r
Deleted:
Deleted: '…i
Deleted:
Deleted: '…r
Deleted:
Deleted: -sid
Deleted: ure
Deleted: E
Deleted:
Deleted:
Deleted: ure
Deleted: F
Deleted:
Deleted:
Deleted: d…
Deleted: ure
Deleted: G
Deleted: ure
Deleted: '…r
Deleted:
Deleted: '…i
Deleted:
Deleted: '…r
Deleted:
Deleted: -s
Deleted: ure
Deleted: E
Deleted: ure
Deleted: F…
Deleted:
Deleted: '…i
Deleted:
Deleted: '…r
Deleted:
Deleted: ure
Deleted: F…
Deleted:
Deleted: '…i
Deleted:

($p < 0.001$) the number of $CRF^+/c\text{-}Fos^+$ neurons compared to their respective controls. The increase in the number of $CRF^+/c\text{-}Fos^+$ neurons was higher ($p < 0.01$) after spontaneous withdrawal versus METH treatment (Fig. 3g).

Effect of chronic methamphetamine administration and withdrawal on markers of sympathetic activity and cellular stress in the heart left ventricle

We examined the effects of chronic METH treatment and withdrawal on the noradrenergic pathways innervating the heart in mice. Two-way ANOVA for S-COMT expression revealed a significant main effect of treatment ($F_{[1,20]} = 8.747$, $p < 0.01$; Fig. 4a). Regarding MB-COMT quantification (Fig. 4b), two-way ANOVA revealed a significant main effect of treatment ($F_{[1,20]} = 11.77$, $p < 0.01$). *Post-hoc* test revealed that chronic MET treatment or spontaneous withdrawal increased S-COMT ($p < 0.05$) and MB-COMT ($p < 0.01$) expression versus their respective control groups in the left ventricle (Fig. 4a, b).

Since TH activity, a marker of catecholamine synthesis, is regulated by phosphorylation of specific serine residues, mainly serine 40 (Dunkley et al. 2004), we have evaluated the levels of this protein in the heart left ventricle of chronic METH-treated and -withdrawn mice. Two-way ANOVA for THpSer40 expression revealed a significant main effect of treatment ($F_{[1,19]} = 5.63$, $p < 0.05$), withdrawal ($F_{[1,19]} = 9.41$, $p < 0.01$), and interaction ($F_{[1,19]} = 9.60$, $p < 0.01$). Holm–Sidak *post-hoc* test showed increased ($p < 0.001$) THpSer40 levels in the METH-withdrawn group compared with the saline-withdrawn group ($p < 0.01$) and the chronic METH-treated group ($p < 0.01$; Fig. 5). Chronic METH did not increase THpSer40 levels ($p > 0.05$).

Expression of Hsp27 and phospho-Hsp27 in chronic methamphetamine treatment and withdrawal

We examined Hsp27 and pHSP27 expression, which is highly expressed in the heart (Latchman 2002), to determine the magnitude and severity of cellular stress during chronic METH treatment and withdrawal. Two-way ANOVA for Hsp27 expression revealed a significant main effect of withdrawal ($F_{[1,21]} = 5.39$, $p < 0.05$). Since we have set a priori hypothesis that METH withdrawal will increase Hsp27 expression, we

Deleted: ure
Deleted: G
Deleted:
Deleted: ‘
Deleted: ’
Deleted:
Deleted: ure
Deleted:
Deleted: A
Deleted: ure
Deleted: B
Deleted: ‘
Deleted: ’
Deleted: -
Deleted: ure
Deleted: A,B
Deleted: ‘
Deleted: ’
Deleted: ‘
Deleted: ’
Deleted: ‘
Deleted: ’
Deleted: -
Deleted: ure
Deleted:
Deleted:
Deleted: -

performed planned comparisons to test this hypothesis. *Post-hoc* analysis revealed that METH withdrawal induced a significant increase in Hsp27 expression in the left ventricle compared with chronic METH-treated group ($p < 0.05$) and a close to significance increase compared with the saline withdrawal group ($p = 0.06$; Fig. 6a). Two-way ANOVA for pHSP27 revealed a significant effect of treatment ($F_{[1,23]} = 24.20, p < 0.001$), withdrawal ($F_{[1,23]} = 16.59, p < 0.001$), and a significant interaction ($F_{[1,23]} = 17.09, p < 0.01$). METH withdrawal significantly enhanced pHSP27 compared to its respective control group ($p < 0.001$), as well as compared to the chronic METH-treated group ($p < 0.01$; Fig. 6b).

Discussion

In the present study, we demonstrated that METH withdrawal induced an increase in CRF immunoreactivity and caused an increase of c-Fos signal in the CRF neurons of PVN and ovBNST. This neurotransmitter changes in the brain were accompanied by alterations of markers of sympathetic heart activation, as shown by an increase in THpSer40, as well as MB- and S-COMT in the left ventricle. No body weight or heart weight/histological changes were observed following chronic METH treatment or withdrawal. There was also evidence of cellular stress in the heart during METH withdrawal as indicated by the increased levels of Hsp27 in the left ventricle.

The role of the ovBNST in the regulation of heart rate has been largely studied. In particular, microinfusion of CRF in this brain region increases heart rate during stress (Nijsen et al. 2001), via CRF1 and CRF2 receptors activation (Oliveira et al. 2015). The PVN has also been clearly identified as essential for the sympathetic activation of the heart (Yu et al. 2016; Deng et al. 2015). We have recently shown that this PVN mediated sympathetic activation is CRF1-dependent and proposed the existence of a plausible loop of CRF–noradrenaline between the PVN and the brainstem (Martinez-Laorden et al. 2014; Garcia-Carmona et al. 2015). CRF and its analogues can also induce sympathetic heart and vasculature effect by increasing the secretion of noradrenaline and adrenaline from the sympathetic nervous system and adrenal medulla, respectively, and play a role within the heart as local mediators (Yang et al. 2010).

Previous reports have demonstrated that drug withdrawal activates the CRF neurons of PVN and thus to modulate the HPA axis activity (Koob and Le Moal 2008).

Deleted:
Deleted: A
Deleted: ‘
Deleted: ’
Deleted: ‘
Deleted: ’
Deleted: ‘
Deleted: ’
Deleted:
Deleted: B
Deleted: -
Deleted: -
Deleted: -
Deleted: ,

However, in a previous study, we showed using an identical METH administration paradigm that chronic administration of METH induced an increase in corticosterone levels, which returned to baseline levels following a 7-day withdrawal period (Georgiou et al. 2016), suggesting a full recovery of METH-induced HPA activation following a 7 day withdrawal period. Although the peripheral arm of the HPA axis might not be involved, in the present study, we found that METH withdrawal increased CRF and c-Fos/CRF-positive neurons in both PVN and ovBNST. Activation of the brain stress system has been associated with elevated anxiety and a negative emotional state characteristic of drug withdrawal (Loogrip et al. 2011). Indeed, we previously showed that a 7-day withdrawal from chronic METH administration induced an anxiogenic phenotype in mice (Georgiou et al. 2016). Although it is not possible to determine a causal relationship between CRF activation in these brain regions and the anxiogenic phenotype, given the role of the CRF system in the PVN and ovBNST in stress regulation, it would be tempted to speculate a possible role of the CRF activation in the PVN and ovBNST in the emergence of these behavioral alterations. In line with our findings, previous studies showed a significant increase of the number of CRF-containing neurons in PVN and ovBNST in morphine- (Nuñez et al. 2010), alcohol- (Sharko et al. 2016), and cocaine-withdrawn (Nobis et al. 2011) animals. Notably, PVN is considered the main source of stress-related neuroendocrine CRF release (Olive et al. 2002) and withdrawal from drugs of abuse result in the dysregulation of the ovBNST neurons via a CRF-mediated mechanism (Francesconi et al. 2009), further supporting the role of the CRF neurotransmission within these brain regions in the modulation of addiction-associated stress/anxiety responses.

It is well established that acute drug administration is able of enhance the expression of c-Fos (Motbey et al. 2012). This activation also takes place even with a stressor such as a needle prick (Kazakova et al. 2000). It is impossible to determine based on the results of the present study alone whether changes in c-Fos, CRF, etc, observed following METH administration are due to repeated METH treatment or due to an acute effect of the last METH injection. Nonetheless, the fact that increases in CRF^{+}/c-Fos^{+} neurons take place a long time (7 days) after the last METH injection and not shortly (1 h) after the last injection of the drug makes it unlikely that alterations in these markers of stress are due to an acute injection of the drug. However, it is more difficult to determine whether the increase in c-Fos following chronic METH administration, an effect not observed following 7 days of withdrawal, is due to the

summation of repeated injections or rather acute METH injection alone and this is indeed a recognized limitation of our findings.

The changes observed in the CRF activation were concomitant with an increase in makers of sympathetic activation such as THpSer40 levels as MB- and S-COMT in the heart following chronic METH treatment and withdrawal, supporting the activation of the sympathetic system within the heart. Interestingly, these alterations were observed at a time point when no alterations in corticosterone levels were observed as demonstrated in an identical METH administration and withdrawal paradigm (Georgiou et al. 2016), thus indicating that the changes observed in the present study are independent of the HPA axis activity. This is of particular interest given the role of CRF in the HPA axis and highlights the presence of distinct CRF regulatory mechanisms in different brain regions. Although COMT activity in the brain has been associated with increased vulnerability for drug abuse including METH, nicotine, and morphine (Li et al. 2004; Beuten et al. 2005; Ersche et al. 2011) and reward processing (Tunbridge et al. 2013), the present study is the first to assess and show a possible role of COMT in the periphery and specifically in the heart following METH administration and withdrawal. In addition to the changes observed in COMT levels, we have also observed METH-induced enhancement of Hsp27 levels and Hsp27 phosphorylation at Ser82 specifically during withdrawal and not following the chronic treatment with the drug. Given the role of Hsp27 in modulating oxidative stress and apoptosis (Mymrikov et al. 2011), this finding suggests that METH withdrawal induces marked cellular stress responses that might be associated with a myocardial damage (Dettmeyer et al. 2009). This increase in Hsp27 levels in the heart might be a compensatory mechanism to counteract METH-induced oxidative stress, since Hsp27 reacts to stress by acting as a chaperone (Ammon-Treiber et al. 2004; Peart and Gross 2006), preventing oxidative damage (Rogalla et al. 1999), acting as an anti-apoptotic molecule to prevent cell death (Mehlen et al. 1997), or regulating actin cytoskeleton reorganization (Robinson et al. 2010). Similar induction of HSP27 has been reported following administration and/or withdrawal of other drugs of abuse (Toth et al. 2010; Dietrich et al. 2007). The mechanism underlining this HSP27 immunoreactivity cannot be determined from this study alone, but given the evidence showing that administration of a selective inhibitor of ERK activation prevented morphine withdrawal-induced Hsp27 phosphorylation at Ser82 (Martínez-Laoden et al. 2012), it is tempting to speculate that the effect of METH withdrawal on Hsp27 might

be regulated through the extracellular signal-regulated protein kinase (ERK) signaling. While it requires further investigation, it is highly plausible that the observed changes within the brain regions associated with sympathetic control of the heart could mediate the observed markers of sympathetic activation in the heart. In support of this, a causal relationship has been observed between CRF1 activation in selected brain regions such as amygdala, ovBNST, and PVN and stress-induced sympathetic activation of the heart (Nijsen et al. 2000; Chu et al. 2004). In addition, we have previously demonstrated that heart sympathetic activation is CRF1-dependent during morphine withdrawal (Martinez-Laorden et al. 2014, Garcia-Carmona et al. 2015), supporting the role of the central CRF in the peripheral alterations in the heart in drug dependent individuals. Chronic METH use has been linked to a variety of cardiovascular complications associated with increased sympathetic activation such as hypertension and cardiomyopathy. Our current results strongly suggest that increases in COMT, TH, and HSP27 in the heart together with the concomitant increase in CRF activation of ovBNST and PVN, regions both known to be associated with cardiovascular regulation, may at least partly play a role in the biology underlining these complications.

Overall, in this study, we demonstrated alterations on markers of cardiac sympathetic activity, central CRF system, and cardiac Hsp levels following chronic METH administration and/or withdrawal, which are addiction phases normally associated with anxiety and stress reactivity (Koob and Volkow 2016). Our findings provide further insight into the specific biological mechanisms underlying the devastating cardiovascular consequences of METH use and abstinence and provide information for potential targets for the development of novel and effective pharmacotherapies for the treatment of the cardiovascular- and stress-related complications associated with METH use and withdrawal. Further work needs to be carried out to verify the role of increased brain CRF signaling on the observed changes in the heart.

Deleted: ,

Deleted: etc

Deleted: O

Deleted:

Deleted:

Acknowledgements

The authors want to thank Dr. Julie Howarth and Ms. Ashleigh Thompson for her assistance with cardiac histopathology.

Funding information

Funding for this study was provided by a Royal Society grant (RG120556; P.I. Alexis Bailey). The sponsors had no involvement in the design of the study and in the collection, analyses, and interpretation of the data nor in the writing of the manuscript and the decision to submit this article for publication.

Compliance with ethical standards

All experimental procedures were conducted in accordance with the UK Animal Scientific Procedures Act (1986).

References

Abekawa, T., Ohmori, T., Koyama T. (1994). Effects of repeated administration of a high dose of methamphetamine on dopamine and glutamate release in rat striatum and nucleus accumbens. Brain Res, 643(1–2), 276–281, DOI: 10.1016/0006-8993(94)90033-7

Ammon-Treiber, S., Grecksch, G., Stumm, R., Riechert, U., Tischmeyer, H., Reichenauer, A., Höllt, V. (2004). Rapid, transient, and dose-dependent expression of hsp70 messenger RNA in the rat brain after morphine treatment. Cell Stress Chaperones 9(2):182–197, DOI: 10.1379/CSC-42.1

Beuten, J., Payne, T.J., Ma, J.Z., Li, M.D. (2005). Significant association of catechol-O-methyl transferase (COMT) haplotypes with nicotine dependence in male and female smokers of two ethnic populations. Neuropsychopharmacology 31: 675–684

Chu, C.P., Qiu, D.L., Kato, K., Kunitake, T., Watanabe, S., Yu, N.S., Nakazato M., Kannan H. (2004). Central stresscopin modulates cardiovascular function through the adrenal medulla in conscious rats. Regul Pept 119: 53–59, 1-2, DOI: 10.1016/j.regpep.2003.12.007

Ciccarone, D. (2011). Stimulant abuse: pharmacology, cocaine, methamphetamine, treatment, attempts at pharmacotherapy. Primary care, 38(1), 41–58, v-vi, DOI: 10.1016/j.pop.2010.11.004

Cubells, J.F., Rayport, S., Rajendran, G., Sulzer, D. (1994). Methamphetamine neurotoxicity involves vacuolation of endocytic organelles and dopamine-dependent intracellular oxidative stress. J Neurosci 14(4), 2260–2271

Deng, X., Feng, X., Li, S., Gao, Y., Yu, B., Li, G. (2015). Influence of the hypothalamic paraventricular nucleus (PVN) on heart rate variability (HRV) in rat hearts via electronic lesion. Biomed Mater Eng 26 Suppl 1:S487–95, DOI: 10.3233/BME-151338

Dettmeyer, R., Friedrich, K., Schmidt, P., Madea, B. (2009). Heroin-associated myocardial damages—conventional and immunohistochemical investigations. Forensic Sci Int 187(1–3):42–46, DOI: 10.1016/j.forsciint.2009.02.014

Dietrich, J.B., Arpin-Bott, M.P., Kao, D., Dirrig-Grosch, S., Aunis, D., Zwiller, J. (2007). Cocaine induces the expression of homer 1b/c, homer 3a/b, and hsp 27 proteins in rat cerebellum. Synapse 61(8):587–94, DOI: 10.1002/syn.20412

Dunkley, P.R., Bobrovskaya, L., Graham, M.E., von Nagy-Felsobuki, E.I., Dickson, P.W. (2004). Tyrosine hydroxylase phosphorylation: regulation and consequences. J Neurochem, 91(5):1025–1043, DOI: 10.1111/j.1471-4159.2004.02797.x

Ersche, K.D., Roiser, J.P., Lucas, M., Domenici, E., Robbins, T.W., Bullmore, E.T. (2011). Peripheral biomarkers of cognitive response to dopamine receptor agonist treatment. Psychopharmacology 214: 779–789, 4, DOI: 10.1007/s00213-010-2087-1

Francesconi, W., Berton, F., Repunte-Canonigo, V., Hagihara, K., Thurbon, D., Lekic, D., Specio, S.E., Greenwell, T.N., Chen, S.A., Rice, K.C., Richardson, H.N., O'Dell, L.E., Zorrilla, E.P., Morales, M., Koob, G.F., Sanna, P.P. (2009). Protracted withdrawal from alcohol and drugs of abuse impairs long-term potentiation of intrinsic excitability in the juxtacapsular bed nucleus of the stria terminalis. J Neurosci 29:5389–5401, 17, DOI: 10.1523/JNEUROSCI.5129-08.2009

Deleted
Deleted
Deleted
Deleted
Deleted
Deleted
Deleted
Deleted
Deleted

Garcia-Carmona, J.A., Milanes, M.V., Laorden, M.L. (2013). Brain stress system response after morphine-conditioned place preference Int J Neuropsychopharmacol, 16(9): 1999–2011, DOI: 10.1017/S1461145713000588

Garcia-Carmona, J.A., Martinez-Laorden, E., Milanes, M.V., Laorden, M.L. (2015). Sympathetic activity induced by naloxone-precipitated morphine withdrawal is blocked in genetically engineered mice lacking functional CRF1 receptor. Toxicol Appl Pharmacol, 283(1):42–49, DOI: 10.1016/j.taap.2015.01.002

Georgiou, P., Zanos, P., Ehteramyan, M., Hourani, S., Kitchen, I., Maldonado, R., and Bailey, A. (2015). Differential regulation of mGlu5 R and MuOPr by priming- and cue-induced reinstatement of cocaine-seeking behaviour in mice. Addict Biol, 20(5): 902–12, DOI: 10.1111/adb.12208

Georgiou, P., Zanos, P., Garcia-Carmona, J.A., Hourani, S., Kitchen, I., Laorden, M.L., Bailey, A. (2016). Methamphetamine abstinence induces changes in u-opioid receptor, oxytocin and CRF systems: association with an anxiogenic phenotype. Neuropharmacology, 105: 520–532, DOI: 10.1016/j.neuropharm.2016.02.012

Gonzales, R., Mooney, L., Rawson, R.A. (2010). The methamphetamine problem in the United States. Ann Rev Pub Health 31: 385–398, 1, DOI: 10.1146/annurev.publhealth.012809.103600

Henry, B.L., Minassian, A., Perry, W. (2012). Effect of methamphetamine dependence on heart rate variability. Addict Biol 17: 648–658, 3, DOI: 10.1111/j.1369-1600.2010.00270.x

Ito, H., Yeo, K.K., Wijetunga, M., Seto, T.B., Tay, K., Schatz, I.J. (2009). A comparison of echocardiographic findings in young adults with cardiomyopathy: with and without a history of methamphetamine abuse. Clin Cardiol 32: 18–22

Kasch, S. (1987). Serum catecholamines in cocaine intoxicated patients with cardiac symptoms. Ann Emerg Med, 16: 481

Deleted
Deleted
Deleted
Deleted
Deleted
Deleted
Deleted
Deleted
Deleted
Deleted
Deleted

Kaye, S., McKetin, R., Duflou, J., Darke, S. (2007). Methamphetamine and cardiovascular pathology: a review of the evidence. Addiction, 102(8), 1204–1211, DOI: 10.1111/j.1360-0443.2007.01874.x

Kazakova, T.B., Barabanova, S.V., Novikova, N.S., Nosov, M.A., Rogers, V.V., Korneva, E.A. (2000). Induction of c-fos and interleukin-2 genes expression in the central nervous system following stressor stimuli. Pathophysiology 7(1):53–61, DOI: 10.1016/S0928-4680(00)00029-8

Kitchen, I., Slowe, S.J., Matthes, H.W., Kieffer, B. (1997). Quantitative autoradiographic mapping of mu-, delta- and kappa-opioid receptors in knockout mice lacking the mu-opioid receptor gene. Brain Res, 778(1):73–88, DOI: 10.1016/S0006-8993(97)00988-8

Koob, G.F. (2010). The role of CRF and CRF-related peptides in the dark side of addiction. Brain Res 1314: 3–14, DOI: 10.1016/j.brainres.2009.11.008

Koob, G.F., Le Moal, M. (2008). Neurobiological mechanisms for opponent motivational processes in addiction. Philos Trans R Soc Lond Ser B Biol Sci, 363(1507): 3113–3123, DOI: 10.1098/rstb.2008.0094

Koob, G.F., Volkow, N.D. (2016). Neurobiology of addiction: a neurocircuitry analysis. Lancet Psychiatry 3(8):760–73, DOI: 10.1016/S2215-0366(16)00104-8

Krasnova, I.N., Cadet, J.L. (2009). Methamphetamine toxicity and messengers of death. Brain Res Rev, 60(2), 379–407, DOI: 10.1016/j.brainresrev.2009.03.002

Latchman, D.S. (2002). Protection of neuronal and cardiac cells by HSP27. Prog Mol Subcell Biol, 28:253–265, DOI: 10.1007/978-3-642-56348-5_14

LaVoie, M.J., Hastings, T.G. (1999). Dopamine quinone formation and protein modification associated with the striatal neurotoxicity of methamphetamine: evidence against a role for extracellular dopamine. J Neurosci, 19(4), 1484–1491

Li, T., Chen, C.K., Hu, X., Ball, D., Lin, S.K., Chen, W. *et al*. (2004). Association analysis of the DRD4 and COMT genes in

Deleted
Deleted
Deleted
Deleted
Deleted
Deleted
Deleted
Deleted
Deleted

methamphetamine abuse. Am J Med Genet B Neuropsychiatr Genet 129B: 120–124, 1, DOI: 10.1002/ajmg.b.30024

Loogrip, M.L., Koob, G.F., Zorrilla, E.P. (2011). Role of corticotropin-releasing factor in drug addiction: potential for pharmacological intervention. CNS Drugs, 25(4): 271–287, DOI: 10.2165/11587790-000000000-00000

Martínez-Laoden, E., Hurle, M.A., Milanés, M.V., Laorden, M.L., Almela, P. (2012). Morphine withdrawal activates hypothalamic–pituitary–adrenal axis and heat shock protein 27 in the left ventricle: the role of extracellular signal regulated kinase. J Pharmacol Exp Ther 342: 665–675, 3, DOI: 10.1124/jpet.112.193581

Martinez-Laorden, E., Garcia-Carmona, J.A., Baroja-Mazo, A., Romecin, P., Atucha, N.M., Milanes, M.V., Laorden, M.L. (2014). Corticotropin-releasing factor (CRF) receptor-1 is involved in cardiac noradrenergic activity observed during naloxone-precipitated morphine withdrawal. Br J Pharmacol, 171(3):688–700, DOI: 10.1111/bph.12511

Mehlen, P., Mehlen, A., Godet, J., Arrigo, A.P. (1997). Hsp27 as a switch between differentiation and apoptosis in murine embryonic stem cells. J Biol Chem 272:31657–31665, 50, DOI: 10.1074/jbc.272.50.31657

Motbey, C.P., Hunt, G.E., Bowen, M.T., Artiss, S., McGregor, I.S. (2012). Mephedrone (4-methylmethcathinone, 'meow'): acute behavioural effects and distribution of Fos expression in adolescent rats. Addict Biol 17: 409–422, 2, DOI: 10.1111/j.1369-1600.2011.00384.x

Mymrikov, E.V., Seit-Nebi, A.S., Gusev, N.B. (2011). Large potentials of small heat shock proteins. Physiol Rev 91(4):1123–59, DOI: 10.1152/physrev.00023.2010

Nash, J.F., Yamamoto, B.K. (1992). Methamphetamine neurotoxicity and striatal glutamate release: comparison to 3,4-methylenedioxymethamphetamine. Brain Res, 581(2), 237–243, DOI: 10.1016/0006-8993(92)90713-J

Nijsen, M.J., Croiset, G., Stam, R., Bruinjnzeel, A., Diamant, M., de Wied, D.et al. (2000). The role of the CRH type 1 receptor in autonomic responses to corticotropin-releasing hormone in the rat.

Deleted

Deleted

Deleted

Deleted

Deleted

Deleted

Deleted

Neurophsychopharmacology 22: 388–399, 4, DOI: 10.1016/S0893-133X(99)00126-8

Nijsen, M.J., Croiset, G., Diamant, M., De Wied, D., Wiegant, V.M. (2001). CRH signalling in the bed nucleus of the stria terminalis is involved in stress-induced cardiac vagal activation in conscious rats. Neuropsychopharmacology 24(1):1–10, DOI: 10.1016/S0893-133X(00)00167-6

Nobis, W.P., Kash, T.L., Silberman, Y., Winder, D.G. (2011). β-Adrenergic receptors enhance excitatory transmission in the bed nucleus of the stria terminalis through a corticotrophin-releasing factor receptor-dependent and cocaine-regulated mechanism. Biol Psychiatry 69(11):1083–1090, DOI: 10.1016/j.biopsych.2010.12.030

Nuñez, C., Martín, F., Földes, A., Laorden, M.L., Kovács, K.J., Milanés, M.V. (2010). Induction of FosB/ΔFosB in the brain stress system-related structures during morphine dependence and withdrawal. J Neurochem 114: 475–487, 2, DOI: 10.1111/j.1471-4159.2010.06765.x

O'Dell, S.J., Weihmuller, F.B., Marshall, J.F. (1991). Multiple methamphetamine injections induce marked increases in extracellular striatal dopamine which correlate with subsequent neurotoxicity. Brain Res, 564(2), 256–60, DOI: 10.1016/0006-8993(91)91461-9

Olive, M.F., Koenig, H.N., Nannini, M.A., Hodge, C.W. (2002). Elevated extracellular CRF levels in the bed nucleus of the stria terminalis during ethanol withdrawal and reduction by subsequent ethanol intake. Pharmacol Biochem Behav 72:213–220, 1-2, DOI: 10.1016/S0091-3057(01)00748-1

Oliveira, L.A., Almeida, J., Benini, R., Crestani, C.C. (2015). CRF1 and CRF2 receptors in the bed nucleus of the stria terminalis modulate the cardiovascular responses to acute restraint stress in rats. Pharmacol Res, 95-96: 53–62, DOI: 10.1016/j.phrs.2015.03.012

Ongur, D., An, X., Price, J.L. (1998). Prefrontal cortical projections to the hypothalamus in macaque monkeys. J Comp Neurol 401: 480–505, 4,

Deleted

Deleted

Deleted

Deleted

Deleted

DOI: 10.1002/(SICI)1096-9861(19981130)401:4<480::AID-CNE4>3.0.CO;2-F

Panenka, W.J., Procyshyn, R.M., Lecomte, T., MacEwan, G.W., Flynn, S.W., Honer, W.G., Barr, A.M. (2013). Methamphetamine use: a comprehensive review of molecular, preclinical and clinical findings. Drug Alcohol Depend, 129(3), 167–179, DOI: 10.1016/j.drugalcdep.2012.11.016

Peart, J.N., Gross, G.J. (2006). Cardioprotective effects of acute and chronic opioid treatment are mediated via different signaling pathways. Am J Physiol Heart CircPhysiol 291:1746–1753

Risold, P.Y., Swanson, L.W. (1997). Connections of the rat lateral septal complex. Brain Res Rev 24: 115–195, 2-3, DOI: 10.1016/S0165-0173(97)00009-X

Robinson, A.A., Dunn, M.J., McCormack, A., dos Remedios, C., Rose, M.L. (2010). Protective effect of phosphorylated Hsp27 in coronary arteries through actin stabilization. J Mol Cell Cardiol 49: 370–379, 3, DOI: 10.1016/j.yjmcc.2010.06.004

Rogalla, T., Ehrnsperger, M., Preville, X., Kotlyarov, A., Lutsch, G., Ducasse, C., Paul, C., Wieske, M., Arrigo, A.P., Buchner, J., Gaestel, M. (1999). Regulation of Hsp27 oligomerization, chaperone function, and protective activity against oxidative stress/tumor necrosis factor alpha by phosphorylation. J BiolChem 274:18947–18956

Sawchenko, P.E., Swanson, L.W. (1982). Immunohistochemical identification of neurons in the paraventricular nucleus of the hypothalamus that project to the medulla or to the spinal cord in the rat. J Comp Neurol 205: 260–272, 3, DOI: 10.1002/cne.902050306

Sharko, A.C., Kaigler, K.F., Fadel, J.R., Wilson, M.A. (2016). Ethanol-induced anxiolysis and neuronal activation in the amygdala and bed nucleus of the stria terminalis. Alcohol, 50: 19–25, DOI: 10.1016/j.alcohol.2015.11.001

Stamatakis, A.M., Sparta, D.R., Jennings, J.H., McElligott, Z.A., Decot, H., Stuber, G.D. (2014). Amygdala and bed nucleus of the stria terminalis circuitry: implications for addiction-related behaviors.

Deleted
Deleted
Deleted
Deleted
Deleted
Deleted
Deleted
Deleted
Deleted

Neuropharmacology 76:320–328, DOI: 10.1016/j.neuropharm.2013.05.046

Stephans, S.E., Yamamoto, B.K. (1994). Methamphetamine-induced neurotoxicity: roles for glutamate and dopamine efflux. Synapse, 17(3), 203–209, DOI: 10.1002/syn.890170310

Sulzer, D., Sonders, M.S., Poulsen, N.W., Galli, A. (2005). Mechanisms of neurotransmitter release by amphetamines: a review. Prog Neurobiol, 75(6): 406–433, DOI: 10.1016/j.pneurobio.2005.04.003

Toth, M.E., Gonda, S., Vigh, L., Santha, M. (2010). Neuroprotective effect of small heat shock protein, Hsp27, after acute and chronic alcohol administration. Cell Stress Chaperones 15(6):807–17, DOI: 10.1007/s12192-010-0188-8

Tunbridge, E.M., Huber, A., Farrell, S.M., Stumpenhorst, K., Harrison, P.J., Walton, M.E. (2013). The role of cateho-o-methyltransferase in reward processing and addiction. CNS Neurol Disord Drug Targets 11: 306–323

Wada, K. (2011). The history and current state of drug abuse in Japan. Ann N Y Acad Sci, 1216, 62–72, 1, DOI: 10.1111/j.1749-6632.2010.05914.x

Wagner, G.C., Ricaurte, G.A., Seiden, L.S., Schuster, C.R., Miller, R.J., Westley, J. (1980). Long-lasting depletions of striatal dopamine and loss of dopamine uptake sites following repeated administration of methamphetamine. Brain Res, 181(1), 151–160, DOI: 10.1016/0006-8993(80)91265-2

Wiechelman, K.J., Braun, R.D., Fitpatrick, J.D. (1988). Investigation of the bicinchoninic acid protein assay: identification of the groups responsible for color formation. Anal Biochem 175: 231–237, 1, DOI: 10.1016/0003-2697(88)90383-1

Yamamoto, B.K., Zhu, W. (1998). The effects of methamphetamine on the production of free radicals and oxidative stress. J Pharmacol Exp Ther, 287(1), 107–114

Yang, L.Z., Tovote, P., Rayner, M., Kockskämper, J., Pieske, B., Spiess, J. (2010). Corticotropin-releasing factor receptors and urocortins, links

between the brain and the heart. Eur J Pharmacol 632:1–6, 1-3, DOI: 10.1016/j.ejphar.2010.01.027

Yu, Y., Wei, S.G., Zhang, Z.H., Weiss, R.M., Felder, R.B. (2016). ERK1/2 MAPK signaling in hypothalamic paraventricular nucleus contributes to sympathetic excitation in rats with heart failure after myocardial infarction. Am J Physiol Heart Circ Physiol, 310(6):H732–9, DOI: 10.1152/ajpheart.00703.2015

Fig. 1 Microscopic heart histology staining. Mice received one daily injection of saline or methamphetamine (METH; 2 mg/kg; i.p.) and were let to spontaneous withdraw for a period of 7 days. Images represent immunohistochemical hematoxylin-eosin staining of myocardiocytes from **a** chronic saline, **b** chronic METH, **c** saline withdrawal, and **d** METH withdrawal. Scale bar 50 µm. **e** Effect of saline or methamphetamine(METH) treatment on body weight gain in mice. **f** Effect of chronic methamphetamine treatment or withdrawal on the terminal heart weight. Data are the mean ± SEM. Repeated measures two-way ANOVA (**e**) and two-way ANOVA (**f**)

Fig. 2 Effect of chronic METH administration and withdrawal on number of CRF^+, c-Fos^+, and c-Fos^+/CRF^+ neurons in the paraventricular nucleus of the hypothalamus (PVN). Increased c-Fos (c-Fos^+) in corticotropin-releasing factor (CRF^+) neurons in methamphetamine (METH) treated groups in the PVN. Representative immunohistochemical images of c-Fos^+/CRF^+ neurons in the PVN from **a** chronic saline-, **b** saline-withdrawn, **d** chronic METH-treated, and **d** METH-withdrawn mice (scale bar 100 µm). Red arrows = c-Fos^+/CRF^+ neurons; black arrows = CRF^+ neurons; green arrows = c-Fos^+. Quantitative immunohistochemical analysis of **e** CRF^+, **f** c-Fos^+, and **g** c-Fos^+/CRF^+ neurons in the PVN of mice treated with a 10-day steady-dose METH administration paradigm and in mice-withdrawn for 7 days. Data are expressed as mean ± S.E.M. $^{***}p < 0.001$ versus saline withdrawal; $^{++}p < 0.01$, $^{+++}p < 0.001$ versus chronic METH treatment; $^{\&\&}p < 0.01$, $^{\&\&\&}p < 0.001$ versus chronic saline treatment. Two-way ANOVA followed by Holm–Sidak *post-hoc* test (color figure online)

Fig. 3 Effect of chronic METH administration and withdrawal on the number of CRF, c-Fos and c-Fos/CRF neurons in the bed nucleus of the stria terminalis (ovBNST). Increased c-Fos (c-Fos^+) in corticotropin-releasing factor (CRF^+) neurons in

Deleted

Deleted: ure
Deleted: .
Deleted:
Deleted:
Deleted:
Deleted: hae
Deleted: (A)
Deleted: (B)
Deleted: (C)
Deleted: (D)
Deleted: (E)
Deleted: (F)
Deleted: 1E
Deleted:
Deleted: 1F
Deleted: .
Deleted: ure
Deleted: .
Deleted: (A)
Deleted: (B)
Deleted: (C)
Deleted: (D)
Deleted: S
Deleted: :
Deleted: (E)
Deleted: (F)
Deleted: (G)
Deleted:
Deleted:
Deleted:
Deleted:
Deleted: -
Deleted: .
Deleted: ure
Deleted: .

methamphetamine (METH)-treated groups in the mice. Representative immunohistochemical images of c-Fos$^+$/CRF$^+$ neurons in the PVN from **a** chronic saline-, **b** saline-withdrawn, **c** chronic METH-treated, and **d** METH-withdrawn mice (scale bar 100 µm). Red arrows = c-Fos$^+$/CRF$^+$ neurons; black arrows = CRF$^+$ neurons; green arrows = c-Fos$^+$. Quantitative immunohistochemical analysis of **e** CRF$^+$, **f** c-Fos$^+$, and **g** c-Fos$^+$/CRF$^+$ neurons in the PVN of mice treated with a 10-day steady-dose METH administration paradigm and in mice-withdrawn for 7 days. Data are expressed as mean ± S.E.M. ***$p < 0.001$ versus saline withdrawal; $^{++}p < 0.01$, $^{+++}p < 0.001$ versus chronic METH treatment; $^{\&\&}p < 0.01$, $^{\&\&\&}p < 0.001$ versus chronic saline treatment. Two-way ANOVA followed by Holm–Sidak *post-hoc* test (color figure online)

Fig. 4 COMT levels following chronic methamphetamine administration and withdrawal. Western-blotting analysis of **a** soluble-COMT (S-COMT) and **b** membrane-COMT (MB-COMT) in the left ventricle of chronic methamphetamine (METH) or withdrawn mice and their respective saline (Sal) controls. Immunoreactivity of S-COMT or MB-COMT is expressed as a percentage of control (defined as 100%). Data are the mean ± SEM. *$p < 0.05$,**$p < 0.01$ versus saline withdrawal; $^{\&}p < 0.05$, $^{\&\&}p < 0.01$ versus chronic saline treatment. Two-way ANOVA followed by Holm–Sidak *post-hoc* test

Fig. 5 THpSer40 levels following chronic methamphetamine administration and withdrawal. Western-blotting analysis of tyrosine hydroxylase phosphorylated at serine 40 (THpSer40) in the left ventricle of chronic methamphetamine (METH) or withdrawn mice and their respective saline (Sal) controls. Immunoreactivity of THpSer40 is expressed as a percentage of control (defined as 100%). Data are the mean ± SEM. $^{***}p < 0.001$ versus saline withdrawal; $^{++}p < 0.01$ versus chronic METH treatment. Two-way ANOVA followed by Holm–Sidak *post-hoc* test

Fig. 6 Hsp27 and phosphor-Hsp27 levels following chronic methamphetamine administration and withdrawal. Western-blotting analysis of total **a** Hsp27 (Hsp27) and **b** phospho-Hsp27 (pHsp27) in the left ventricle in chronic methamphetamine (METH) or withdrawn mice and their respective controls treated with saline (Sal). Immunoreactivity of Hsp27 or pHsp27 is expressed as a percentage of control (defined as 100%). Data are the mean ± SEM. ***$p < 0.001$ versus saline withdrawal; $^{+}p < 0.05$, $^{++}p < 0.01$ versus chronic METH treatment. Two-way ANOVA followed by Holm–Sidak *post-hoc* test

Deleted:
Deleted: (A)
Deleted: (B)
Deleted: (C)
Deleted: (D)
Deleted: S
Deleted: :
Deleted: (E)
Deleted: (F)
Deleted: (G)
Deleted:
Deleted:
Deleted:
Deleted:
Deleted:
Deleted: -
Deleted: .
Deleted: ure
Deleted: .
Deleted: (A)
Deleted: (B)
Deleted:
Deleted: -
Deleted: .
Deleted: ure
Deleted: :
Deleted:
Deleted: -
Deleted: .
Deleted: ure
Deleted: :
Deleted: (A)
Deleted: (B)
Deleted:
Deleted:
Deleted: -
Deleted: .

FIGURE 1

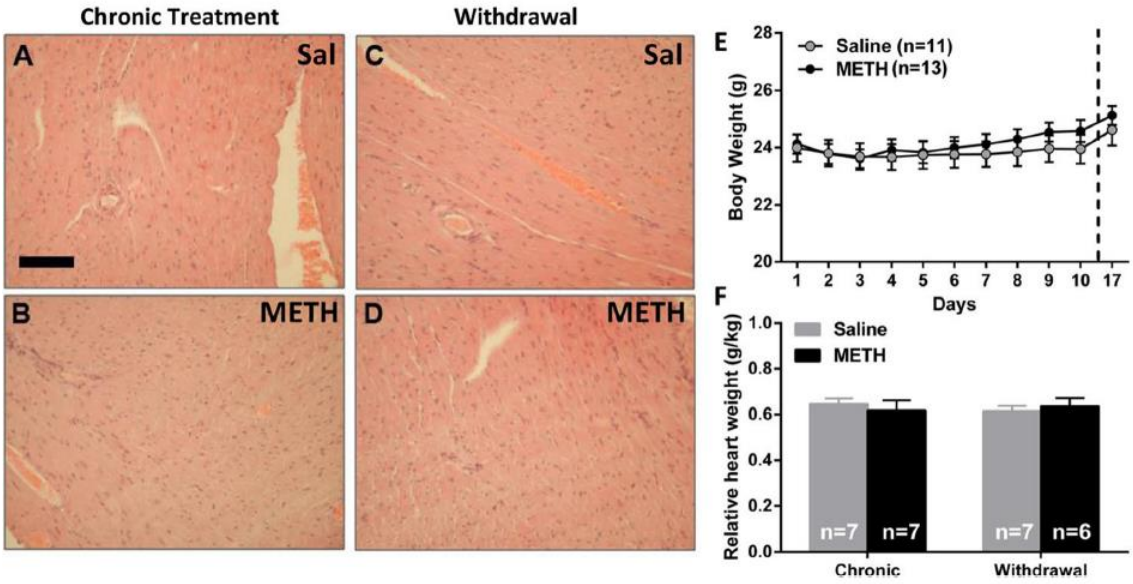

FIGURE 2

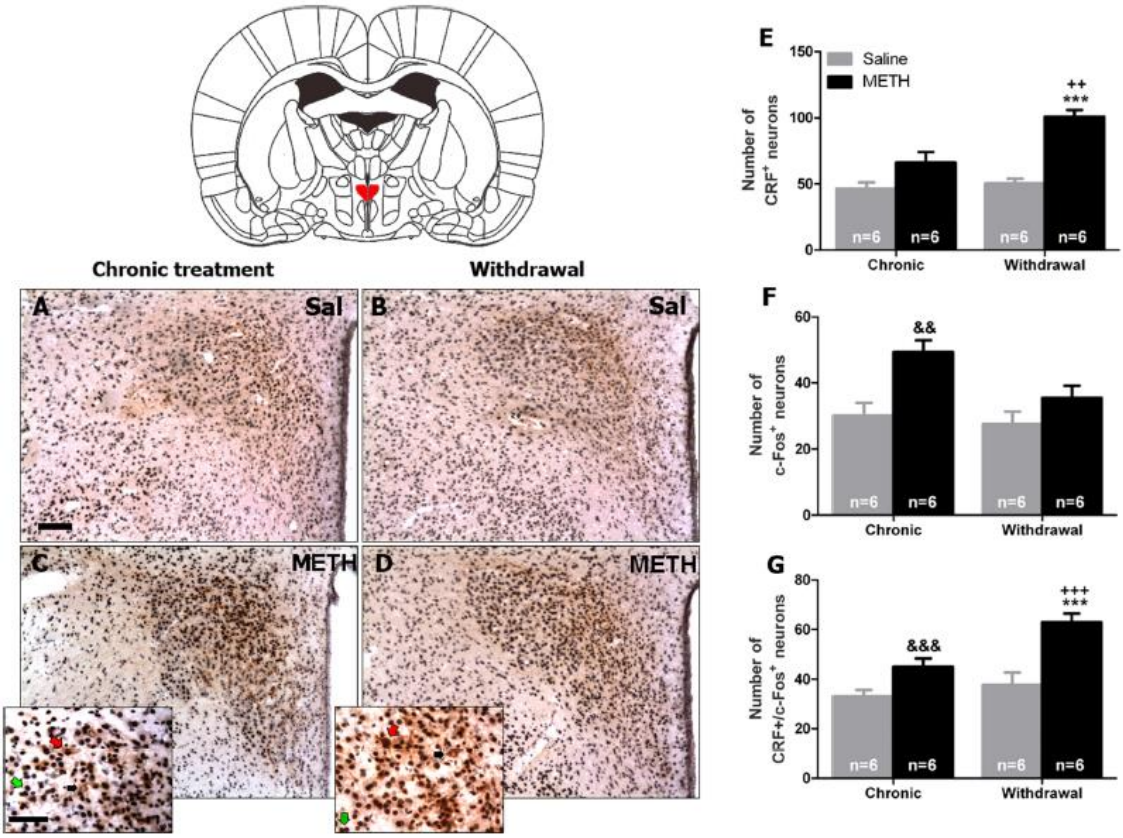

FIGURE 3

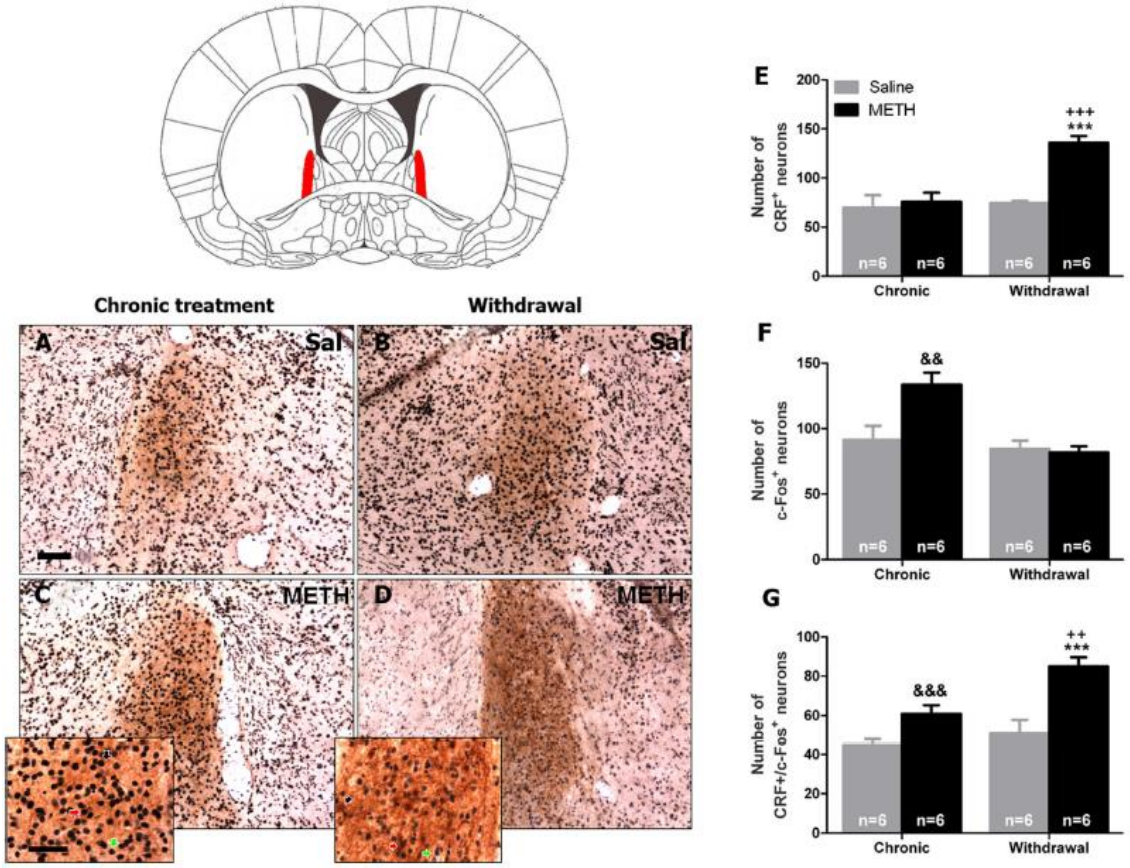

FIGURE 4

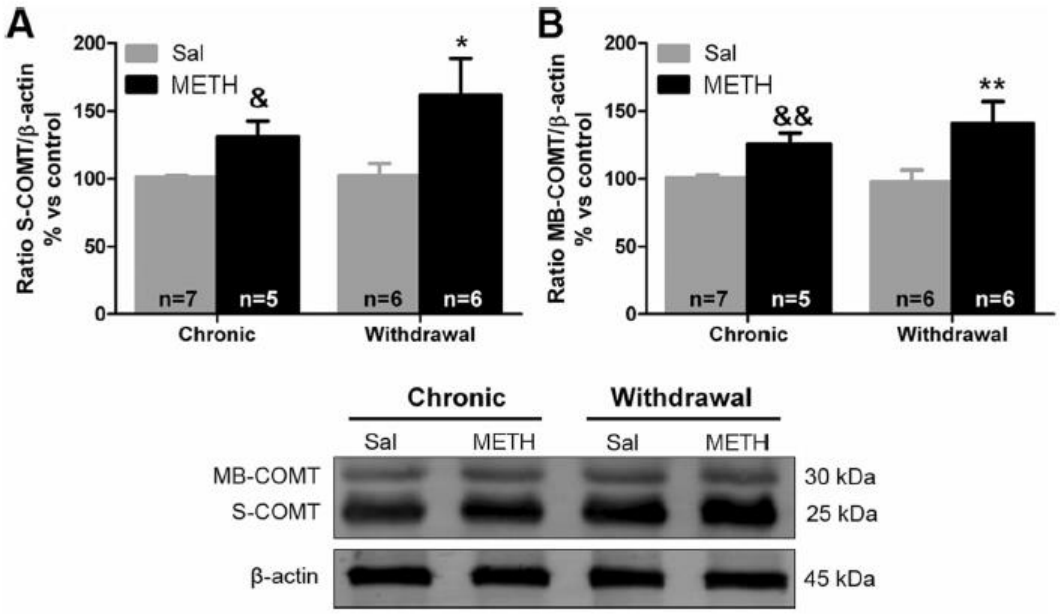

FIGURE 5

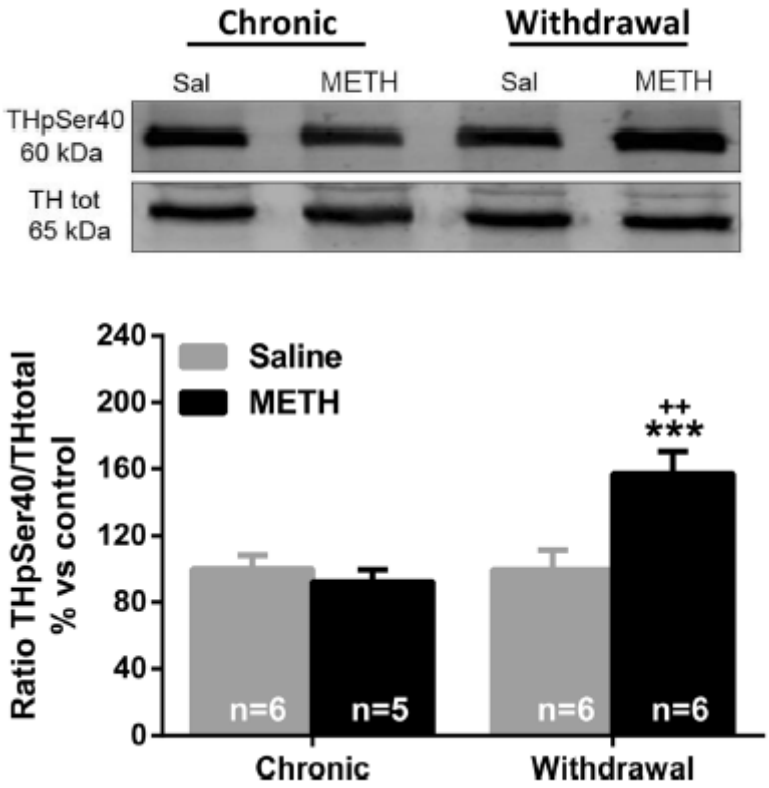

FIGURE 6